IEEE Access
Multidisciplinary | Rapid Review | Open Access Journal

Received March 8, 2019, accepted April 4, 2019, date of publication May 10, 2019, date of current version June 6, 2019.

Digital Object Identifier 10.1109/ACCESS.2019.2916087

A Novel Self-Tuning Fuzzy Logic Controller Based Induction Motor Drive System: An Experimental Approach

NABIL FARAH[1], MD. HAIRUL NIZAM TALIB[1], NOR SHAHIDA MOHD SHAH[2], QAZWAN ABDULLAH[2], ZULKIFILIE IBRAHIM[1], JURIFA BINTI MAT LAZI[1], AND AUZANI JIDIN[1], (Member, IEEE)

[1]Faculty of Electrical Engineering, Universiti Teknikal Malaysia Melaka, Durian Tunggal 76100, Malaysia
[2]Faculty of Engineering Technology, Universiti Tun Hussein Onn Malaysia, Muar 84600, Malaysia

Corresponding authors: Nabil Farah (nabil-farah11@hotmail.com) and Md. Hairul Nizam Talib (hairulnizam@utem.edu.my)

This work was supported in part by the Universiti Teknikal Malaysia Melaka (UTeM) and the Ministry of Education (MOE), Malaysia, under Grant FRGS/1/2015/TK04/FKE/02/F00258, and in part by the Universiti Tun Hussein Onn Malaysia (UTHM) under Grant TIER 1 vot H243.

ABSTRACT High-performance induction motor (IM) drives require fast dynamic responses, robust to parameter variations, withstand load disturbance, stable control systems, and support easy hardware/software implementation. Fuzzy logic control (FLC) for speed controllers is garnering attention from researchers, since it is proven to produce better results compared with the conventional PI speed controllers. However, fixed parameter FLC experiences performance degradation when the system operates away from the design point or is affected by parameter variations or load disturbances. The purpose of this paper is to design and implement a simple self-tuning fuzzy logic controller (ST-FLC) for IM drives application. The proposed self-tuning mechanism is able to adjust the output scaling factor of the main FLC speed controller by improving the accuracy of the crisp output. The IM drive employed an indirect field-oriented control (IFOC) method fed by a hysteresis current controller (HCC). The fixed parameter FLC for the main speed controller comprises nine rules that are tuned to achieve the best performance. Then, a simple self-tuning mechanism is applied to the main fuzzy logic speed controller. All simulation work was done using Simulink and fuzzy tools in the MATLAB software. The effectiveness of the proposed controller was investigated by conducting a comparative analysis between fixed parameter FLC and ST-FLC in forward and reverse speed operations, with and without load disturbances. Finally, the experimental testing was carried out to validate the simulation results with the aid of a digital signal controller board, dSPACE DS1104, with an induction motor drive system. Based on the results, the ST-FLC showed superior performance in transient and steady-state conditions in terms of various performance measures, such as overshoot, rise time, settling time, and recovery time.

INDEX TERMS Induction motor, vector control, speed controller, fuzzy logic controller, self-tuning, dSPACE DS1104, scaling factor.

I. INTRODUCTION

Vector control of induction motor (IM) drives has been implemented in various industrial applications. The essential feature of this control method is the ability to decouple the control of magnetic flux and torque generated by the stator current [1]. This makes the control of induction motor drives more similar to the control of a separately excited DC motor. The performance of vector control of IM drives is sensitive to the variations in the motor parameters. The differences between measured and actual motor parameters usually leads to a deterioration of the dynamic torque response and detunes overall drive performance [2]–[4].

Based on these detuning effects, many researchers have focused on developing accurate mathematical models of the IM with various reference frames [5], [6], such as the stationary reference frame, rotary reference frame, and synchronous reference frame. The synchronous reference frame is most

The associate editor coordinating the review of this manuscript and approving it for publication was Ning Sun.

commonly used to model the IM. These reference frames only deal with the motor parameters. However, other perturbations affect the drive performance such as load disturbance, controller parameters and motor inertia. [7].

The vector control method is normally achieved using a PI speed controller. However, a constant parameter controller is unable to sufficiently control the drives at extreme speeds and parameter variations, and load demands. Therefore, the controller parameters should be continuously adapted based on the current situation or system status. Various adaptation mechanisms have been designed to settle these issues. However, because of their design complexities, few have been successfully applied in the vector control of IM drives [8], [9].

Stringent mathematical modeling is insufficient to handle machine issues. Fuzzy Logic (FL) has been presented as a supplement to the traditional stringent approaches. The complex mathematical model can be integrated into a Fuzzy Logic controller (FLC) using linguistic rules. In the past few years, researchers have begun to investigate the possibility of FLC as a speed controller for induction motor drives [10]–[14]. Various methods have been used to design fuzzy logic speed controllers in motor drives.

Some methods are concerned with enhancing the design and behavior of the standard fixed parameters FLC [13], [15]. The standard FLC comprises a set of rules, membership functions, and scaling factors. These parameters are constant and optimized under rated conditions. Other methods combined the features of FLC with adaptation mechanisms such as the Model Reference Adaptive System (MRAS) and Sliding Mode Control (SMC) in order to enhance the drive performance under heavy motor parameters variations and various operating ranges [16].

A fuzzy rules reduction and membership functions optimization was proposed in [17] to enhance the speed performance. However, the performance investigations were limited to simulation results with no experimental validations. A fuzzy logic scaling factor determination was studied in [18] utilizing the sliding mode method.

Fuzzy scaling factors were found to have severe influence on the system's overall performance. Fixed fuzzy scaling factors might result in degraded performances under heavy perturbations. Scaling factors determination or tuning might be affected by parameter variations and load disturbances. To solve this issue, self-tuning based fuzzy scaling factors have been proposed. This mechanism can update the scaling factors in accordance with the current trend of the system's conditions. Past research literature have focused on developing self-tuning approaches to tune the fuzzy scaling factors online accordingly. A Simplified Fuzzy Logic Controller in [19] was used to tune the output scaling factor of the main speed FLC. The simplified FLC rules reduced the system's computational burden. FLC speed controller scaling factors were tuned based on MRAS and Takagi-Sugeno fuzzy type [20]. System complexity and the higher number of fuzzy rules were proved to increase the system's computational burden [21], especially during hardware implementation.

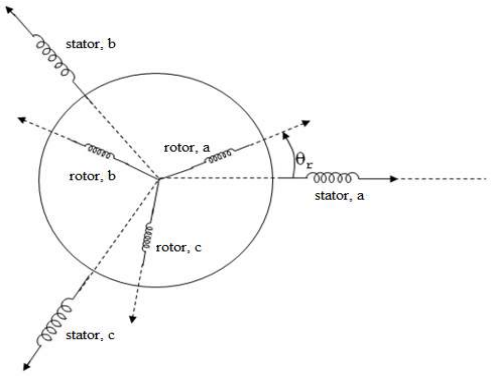

FIGURE 1. Three-phase of equivalent phasor diagram.

A survey of the literature indicates that few studies focus on Self-Tuning of fuzzy scaling factors with experimental investigations. The drawbacks of existing Self-Tuning of fuzzy scaling factors are their complexity and the large number of fuzzy rules which lead to a very high computational burden on the drive system. The use of additional FLC to tune the main FLC or other mechanisms such as MRAS and Sliding Mode Control (SMC) results in an increment on the system's computational burden.

This research tries to create a balance between the system's computational burdens and improved system performance. We propose a simple but effective Self-Tuning FLC (ST-FLC) method, where the controller gain is adjusted continuously with the help of gain updating factor. In our method, we focused only on the tuning of output Scaling Factor (SF), considering it as equivalent to the controller gain. Tuning of the output SF has been given the highest priority because of its severe influence on the performance and stability of the system. Mudi *et al.* [22] has fairly pointed out this matter. In our method, the main FLC is tuned on-line (during operation) by dynamically adjusting its output SF by a gain updating factor β. The value of β is determined from mathematical algorithm based on input change of error Δe which is derived from system expert knowledge. The proposed ST-FLC applied to FLC of IM drive system and compared with standard FLC based on simulation and experiments with various types of operating conditions.

The rest of paper is classified into five sections: Section II details the dynamic modeling of IM, Section III describes the speed controller designs, Section IV presents simulation results, section V discusses the stability analysis, section VI reports the experimental results, section VII analyzes the execution time, and finally, Section VIII summarizes the findings and conclusions.

II. IM DYNAMIC MODELLING

The dynamic performance of an AC machine is somewhat complex because the three-phase rotor winding moves with respect to the three-phase stator winding, as shown in Fig. 1. Basically, it can be viewed as a transformer with a moving

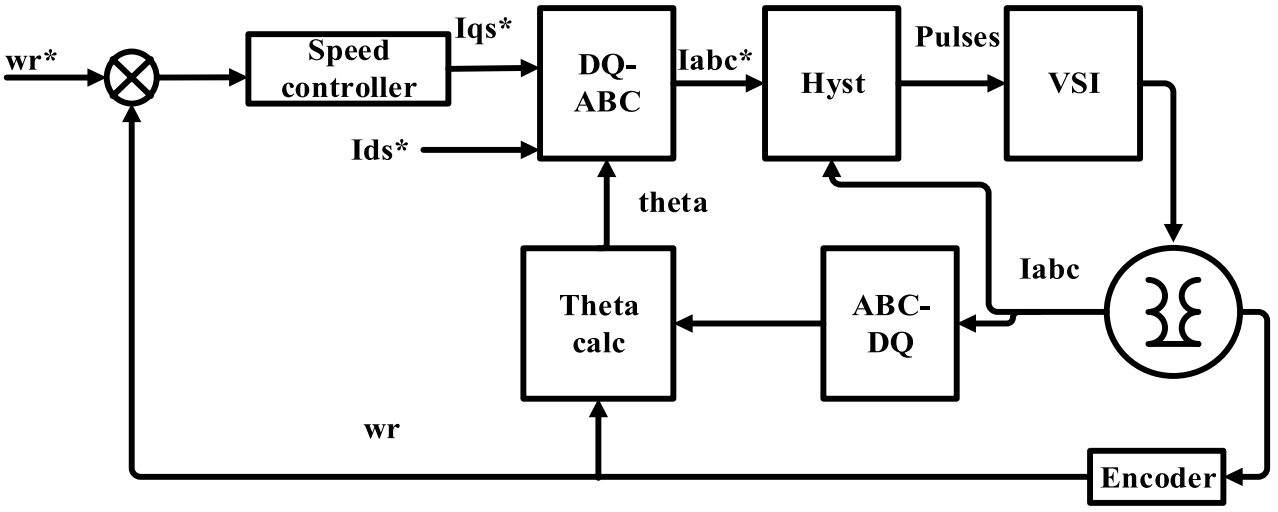

FIGURE 2. Configuration of IFOC for IM drives.

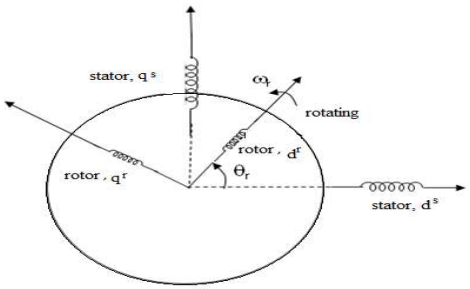

FIGURE 3. Two-phase of equivalent phasor diagram.

secondary winding, where the coupling coefficient between the stator and rotor phases change continuously with the change of rotor position. The three-phase machine can be represented by an equivalent two-phase machine (Fig. 3) where *ds* and *qs* correspond to stator direct and quadrature axis. Meanwhile *dr* and *qr* correspond to rotor direct and quadrature axis.

The diagram of the drive discussed in this study is presented in Fig. 2. The drive utilized the Indirect Field Oriented Control (IFOC) with a squirrel cage IM by means of a hysteresis current controller [23]–[25]. Under ideal IFOC conditions, the rotor flux linkage is oriented along the d-axis of the motor. The mathematical model of the IM is represented in synchronous reference frame expressed as the following equation:

$$v_{sd} = R_s I_{sd} + \frac{d\varphi_{sd}}{dt} - \omega_s \varphi_{sq} \quad (1)$$

$$v_{sq} = R_s I_{sq} + \frac{d\varphi_{sq}}{dt} + \omega_s \varphi_{sd} \quad (2)$$

$$v_{rd} = R_r I_{rd} + \frac{d\varphi_{rd}}{dt} - (\omega_s - \omega_r)\varphi_{rq} \quad (3)$$

$$v_{rq} = R_r I_{rq} + \frac{d\varphi_{rq}}{dt} + (\omega_s - \omega_r)\varphi_{rd} \quad (4)$$

Flux equations:

$$\varphi_{sd} = L_{ls} I_{sd} + L_m I_{rd} \quad (5)$$

$$\varphi_{sq} = \mathrm{L_{ls} I_{sq}} + \mathrm{L_m I_{rq}} \quad (6)$$

$$\varphi_{rd} = \mathrm{L_m I_{sd}} + \mathrm{L_{lr} I_{rd}} \quad (7)$$

$$\varphi_{rq} = \mathrm{L_m I_{sq}} + \mathrm{L_{lr} I_{rq}} \quad (8)$$

where v_{sd}, v_{sq} are the applied voltages to the stator I_{sd}, I_{sq}, I_{rd}, I_{rq} are the corresponding d and q axis stator current and rotor currents.φ_{sd}, φ_{sq}, φ_{rd}, φ_{rq} are the stator and rotor flux component. $\mathrm{R_s}$, $\mathrm{R_r}$ are the stator and rotor resistances .L_{ls}, L_{lr} denotes stator and rotor inductances, whereas $\mathrm{L_m}$ is the mutual inductance.

Combining the flux equation with (5), (6), (7) and (8), the electrical transient model in terms of voltage and current can be represented in matrix form as:

$$\begin{bmatrix} \mathrm{V_{qs}} \\ \mathrm{V_{ds}} \\ \mathrm{V_{qr}} \\ \mathrm{V_{dr}} \end{bmatrix} = \begin{bmatrix} R_s+\rho L_s & L_s\omega_s & \rho L_m & L_m\omega_s \\ -L_s\omega_s & R_s+\rho L_s & -L_m\omega_s & \rho L_m \\ \rho L_m & L_m(\omega_r-\omega_s) & R_r+\rho L_r & L_r(\omega_r-\omega_s) \\ -L_m(\omega_s-\omega_r) & \rho L_m & -L_r(\omega_s-\omega_r) & R_r+\rho L_r \end{bmatrix} \times \begin{bmatrix} \mathrm{i_{qs}} \\ \mathrm{i_{ds}} \\ \mathrm{i_{qr}} \\ \mathrm{i_{dr}} \end{bmatrix} \quad (9)$$

where ρ is the Laplace operator. The speed ω_r in matrix form cannot normally be treated as a constant. It can be related to torque as:

$$T_e = T_L + J\frac{d\omega_m}{dt} = T_L + \frac{2}{P}J\frac{d\omega_m}{dt} \quad (10)$$

where T_L = load torque, J = rotor inertia, and ω_m = mechanical speed.

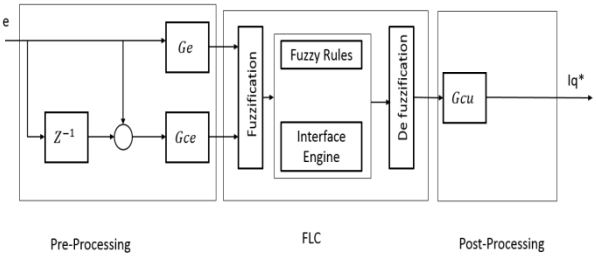

FIGURE 4. Configuration of IFOC for IM drives.

III. SPEED CONTROLLER DESIGN

The proposed ST-FLC method was evaluated with a standard FLC based on 9 rules. The standard FLC and ST-FLC design structures are detailed in this section. The proposed ST-FLC is a mathematical algorithm to tune the output scaling factor based on the input (change of error).

A. STANDARD FLC DESIGN

As illustrated in the following block diagram (Fig. 4), the FLC has three parts - pre-processing, fuzzy rules & interface engine, and post-processing. In the pre-processing part, the fuzzy controller input variables are speed error (e) and change of speed error (Δe). The inputs scaling factors of error and change of error are Ge and Gce respectively.

$$e(k) = G_e\left(\omega_r^*(k)\right) - \omega_r(k) = G_e(k) \tag{11}$$

$$\Delta e(k) = G_{ce}\frac{(e(k) - e(k-1))}{T_{samp}} \tag{12}$$

In the diagram,ω^*_r and ω_r stand for the reference speed and actual speed respectively, while k and $k-1$ represent the current state and past state in order to get the change of speed error. Δe is the change of speed error, and T_{samp} is the sampling time.

The fuzzy input variables are fuzzified into suitable linguistic values, then processed in the fuzzy set region which includes membership function. Fuzzy controllers possess three different variables which have the most impact on their overall performance, namely Scaling Factors (SF), Membership Functions (MF) and fuzzy rules [20].

Different type of MF shapes can be utilized to design the FLC. The most popular types of MF shapes are the triangular and trapezoidal shaped MF [26], [27]. They produce less computational burden in comparison with other shapes. Triangular and Trapezoidal shaped 3x3 MF were used for inputs and outputs parts. The notation for MF is represented by N for Negative, Z for Zero, and P for Positive. The MF was designed using the fuzzy toolbox in the Matlab software as shown in Fig. 5.

In this paper, the well-known min-max fuzzy interface was utilized due to its capabilities in achieving enhanced control performance [28]. The output performance was measured in accordance with the implication and aggregation of the fuzzy output set. The center of gravity (CoG) algorithm was

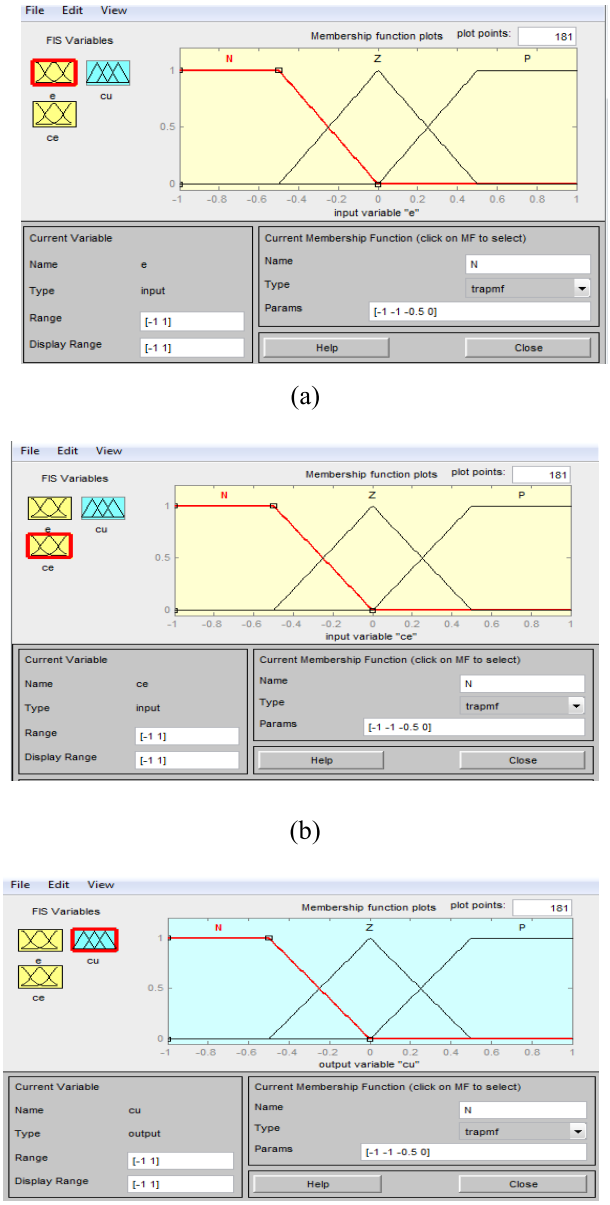

FIGURE 5. 3 × 3 MFs design in MATLAB/SIMULINK, (a) error MF, (b) change of error MF and (c) output fuzzy MF.

utilized to obtain an efficient control signal [29]. The inputs and outputs of FLC qualitative relation were illustrated by designing fuzzy rules sets. IF and THEN conditional states were utilized to represent the fuzzy rules in linguistic terms, where these linguistic terms were used to identify the output fuzzy set. The rules were developed using phase-plane-trajectory method [30] as this approach provides an easy and systematic technique to relate overall dynamic performance of the system with the fuzzy knowledge base. This method was implemented in order to design the rules based on 3x3 membership functions as shown in Table 1.

TABLE 1. Rules base for standard flc (9rules).

e / ∇e	N	Z	P
N	N	N	Z
Z	N	Z	P
P	Z	P	P

The final step of the FLC system is post-processing. The output signal ΔIq was multiplied by the output scaling factors to obtain the following:

$$i^*_{sq}(k) = i^*_{\ sq}(k-1) + G_{cu}\left(\Delta i^*_{sq}(k)\right) \tag{13}$$

Scaling factors are one of the most essential parameters of the FLC due to their critical impact on overall system performance. Initially, the FLC scaling factors were computed in accordance with the maximum value of the speed reference when the motor was running at rated speed. The scaling factor for input fuzzy speed error can be calculated based on the following equation:

$$G_e = \frac{1}{|2\omega_{emax}|} \tag{14}$$

In which the ω_{emax} is the maximum speed error when the motor is operating at rated speed. The constant coefficient 2 was used to ensure the maximum ranges for the forward to reverse speed operation. The rated speed of the induction motor was 149.7 rad/s, hence the input scaling factor of speed error was 0.00334.

In addition, the scaling factor for change of speed error, Gce, can be obtained from the electrical and mechanical torque equations. The maximum torque can be expressed in the following equation:

$$T_{max} = \frac{3}{2}\frac{P}{2}\frac{L_m^2}{L_r} \tag{15}$$

In which the i_{sd}^{max} is the reference flux current component at no load operation and i_{sq}^{max} is the maximum torque current component. The maximum torque current was expected to be twice that of the rated current. The final change of speed error Gce was computed as follows:

$$G_{ce} = \frac{1}{|\Delta\omega_{max}|} = \frac{1}{0.389}$$

This initial value of Gce was based on the rated values of the motor parameters. Hence several simulations steps were performed in order to find the optimum performance. The value of Gce required to obtain zero overshoot and faster settling and rise time was found to be 0.350. The output fuzzy scaling factor Gcu was maintained at 1 for the standard fixed parameters FLC.

B. PROPOSED ST-FLC

The scaling factors have a crucial impact on the overall system performance. This research proposed simple Self-Tuning FLC to tune the output scaling factor, Gcu, in accordance with the input change of speed error, Gce. The proposed Self-Tuning mechanism (ST-FLC) focused on tuning the output SF online based on the change of speed error. The block diagram of the proposed ST-FLC is presented in Fig. 6. The ST-FLC utilized the change of speed error which fed into the ST-FLC algorithm to adjust the output scaling factor of the main FLC. The proposed ST employed a simple computation algorithm in order to reduce system complexity and computational burden.

The ST-FLC scaling factors (*Ge*, *Gce*, and *Gcu*) are related to the inputs and outputs (e, Δe, Δu) in the following equations:

$$e = Ge \times e \tag{16}$$

$$\Delta e = Gce \times \Delta e \tag{17}$$

$$\Delta u = (\beta Gcu) \times \Delta u \tag{18}$$

where:

$$\beta = K_1\left(\frac{1}{m} + |\Delta e|\right) \tag{19}$$

e is the speed error and *Ge* is the input scaling factor for speed error,Δe is change of speed error and *Gce* is the input scaling factor for change of speed error. Δu is the change in output fuzzy and *Gcu* is the output scaling factor for change in output fuzzy. The change of speed error Δe actually indicates the instantaneous process trends in terms of speed of response, while the change of error e only provides instantaneous process trends. Since we concerned about the process trends in terms of speed response, change of speed error Δe is considered for adjusting the output gain.

The variable β is the non-linear gain online updating factor for the output scaling factor (*Gcu*). It is formulated based on expert knowledge of the system according to this concept: *((If the system is moving faster towards its desired operating-point (small Δe), then output action (Δu) needs to be reduced (reduce Gcu) to prevent big overshoot and/or undershoot. In contrast, if the system is rapidly moving away from the desired operating-point (big Δe), then output action (Δu) needs be increased (increase Gcu) for limiting these deviations for a faster recovery of the system to its desired operating point)).* In other words, if the value of Δe is small, then *Gcu* need to be reduced and if Δe is big, then *Gcu* need to be increased. This explained the relationship between the change of error Δe and output scaling factor *Gcu*. Hence, the β value is formulated based on this concept by adding the Δe to the fraction ($\frac{1}{m}$) to avoid lower gain multiplication (Gcu) when the Δe is very small. Lower multiplication of gain may result in oscillation and not stable condition during steady state operation. The value of m is chosen based on the number of uniform input (e and Δe) fuzzy partition (number of MFs) which is 3 in our case. The value of *K1* is chosen to make the possible variation in β which set to 4 based on tuning process.

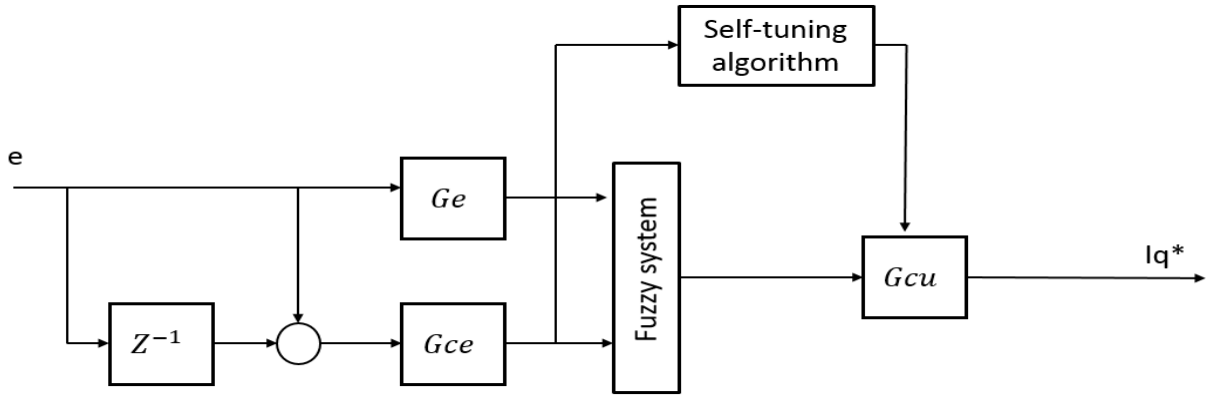

FIGURE 6. Block diagram of the proposed ST-FLC.

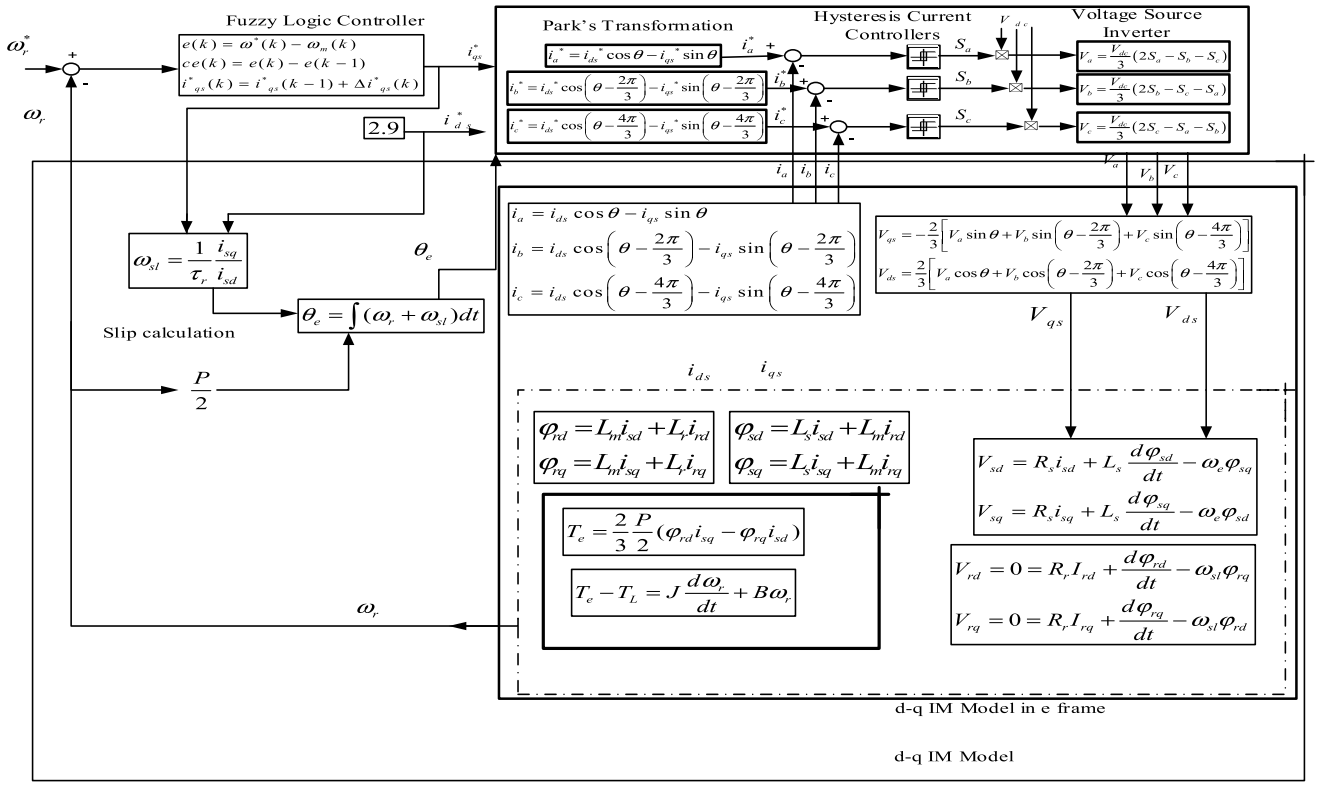

FIGURE 7. Vector control of IM drive.

Other fuzzy parameters were kept unchanged, similar to the standard fixed parameters FLC. The difference between the ST-FLC and standard fixed parameters FLC is that while the standard FLC uses the constant output scaling factor, the ST-FLC utilizes the algorithm β as depicted in equation 20 to tune the output scaling factor online based on the input change of speed error Δe.

IV. SIMULATION SETUP AND RESULT

The IM drive system was designed and simulated by utilizing MATLAB/SIMULINK. Each part of the system was designed separately and then integrated to make the IM drive system. The overall drive model is presented in Fig. 7 and the 3-phase induction motor parameters are presented in Appendix A.

The simulation investigation was carried out based on two speed controllers, a standard 9 rules FLC and the proposed ST-FLC. In the following section, performance comparison is done in terms of speed, torque, and current behaviors of both controllers. The simulation sampling time used was 50μ s for both controllers. The input DC voltage for the hysteresis PWM controller VSI was 537Vdc.

A. NO LOAD OPERATION

The speed performance investigation with no load conditions was performed to ensure the workability of the speed

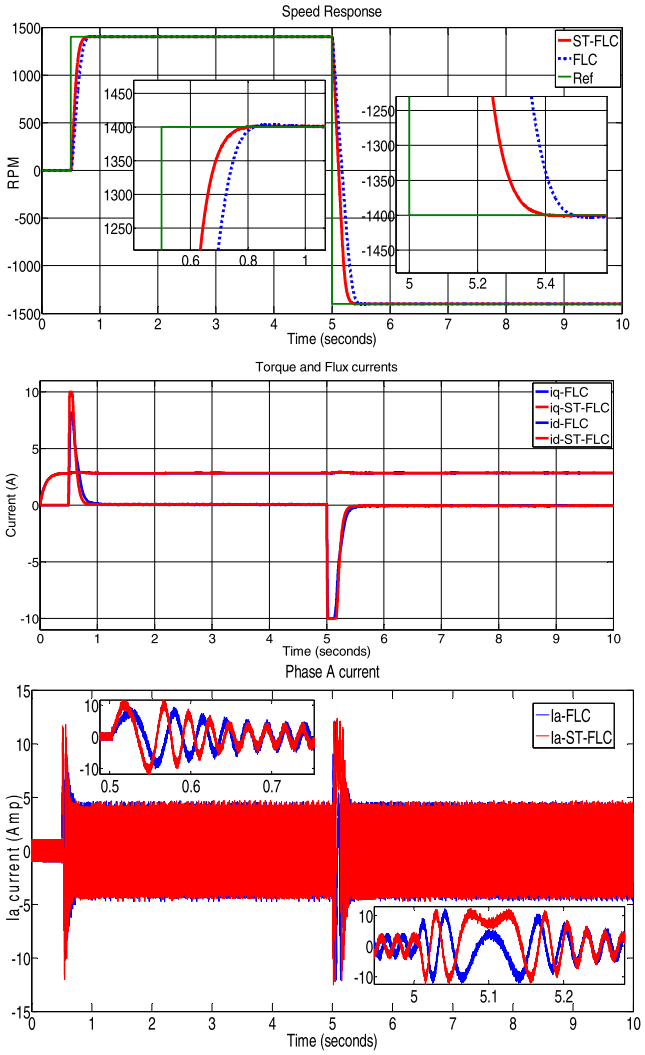

FIGURE 8. Performance comparison of ST-FLC and FLC at 1400rpm no load operations.

controllers. The reference speed was varied from 0.5s at standstill to rated speed operation and reversed to rated negative operation at 5s. Overall, a consistent speed performance for both controllers was obtained during forward and reverse operations. The speed performances of both controllers shown in Fig. 8(a) are summarized in Table 2. The ST-FLC produced better speed performance in comparison to the standard FLC in terms of rise time and settling time. Both controllers obtained almost zero overshoot, which was consistent with the design criteria.

Based on the flux and torque responses in Fig. 8(b), it is proved that the torque and flux current components are decoupled as FOC behavior. It was observed that the ST-FLC reached torque current limits unlike the standard FLC. In addition, ST-FLC had faster torque response. Consequently, the phase A of motor current recorded similar behavior. The current reached 10 A and remained constant until the steady state condition. Interestingly, the steady state

TABLE 2. Performance measures comparison between FLC and ST-FLC.

Operation	Measures	FLC	ST-FLC
Forward	Settling time (s)	0.3238	0.293
	Rise time (s)	0.2412	0.17082
	Overshoot (%)	0.2857	0.0714
Reverse	Settling time (s)	0.432	0.3352
	Rise time (s)	0.2457	0.177268
	Overshoot (%)	0.2643	0.0714

current of the ST-FLC had a lower amplitude (put value) compared to the standard FLC. All current performances were a reflection of speed responses of both controllers.

Further analysis on the steady state current was carried out. Fast Fourier Transform (FFT) analysis was used to compute the Total Harmonics Distortion (THD) produced by stator current. Twenty cycles of the current were selected, starting at 3s, and the frequency limited to 100Hz to obtain a clear view of the THD spectrum. Fig. 9 shows the current and THD spectrum for both controllers and a detailed summary is recorded in Table 3.

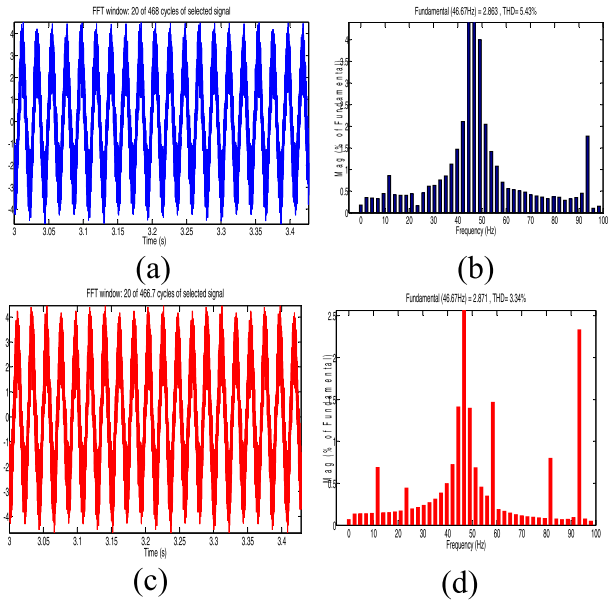

FIGURE 9. THD analysis of phase A current. (a) Ia current (FLC). (b) THD (FLC). (c) Ia current (ST-FLC). (d) THD % (ST-FLC).

TABLE 3. Phase a current THD comparison.

Controller	THD%	Fundamental (46.67Hz)
FLC	5.43	2.863
ST-FLC	3.34	2.871

B. LOAD OPERATIONS

The load rejection capabilities of the controllers were investigated through a load test. A rated load disturbance was applied at 3s when the motor operated at 1400 rpm and at 5s when it reversed its operation. Fig. 10 shows the performance comparison of ST-FLC and FLC for load.

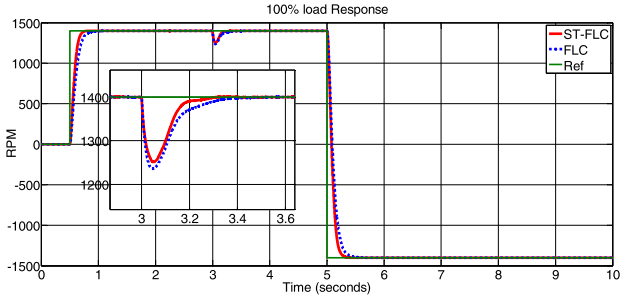

FIGURE 10. ST-FLC and FLC Comparison of load disturbance rejection capabilities.

Situations durging load disturbance operation a speed drop of 120 rpm and 114 rpm for FLC and ST-FLC respectively. The ST-FLC and FLC had a recovery time of 0.201s and 0.341s respectively at 1400 rpm speed operation. The ST-FLC was faster than the standard FLC by 0.24s.

V. STABILITY ANALYSIS

Apart from this, the IM drive system is a closed loop system where the output speed of the motor is fed back to speed controller. In order to analyze the closed loop IM, drive a transfer function of the system must be derived, but the IM drive is a complex system which can be difficult to obtain accurate transfer function of the system. However, the IM drive system can be represented by a second order equation (transfer function) as discussed by [20], [31]. Therefore, a second order equation (transfer function) of the closed loop IM drive with ST-FLC can be obtained by referring to the output speed step response. With the help of control system theory[32], the general equation of transfer function of second order control system is given as:

$$\zeta G(s) = \frac{\omega_n^2}{s^2 + 2\varepsilon\omega_n s + \omega_n^2} \tag{20}$$

where ω_n is the natural frequency and ε is the damping ratio. The percent overshoot of the system can be calculated using:

$$OS\% = e^{-\frac{\varepsilon\pi}{\sqrt{1-\varepsilon^2}}} \tag{21}$$

Rearranging the equation, the ζ can be calculated as:

$$\varepsilon = \frac{-\ln(OS\%/100)}{\sqrt{\pi^2 + In^2(OS\%/100)}} \tag{22}$$

The settling time formula is:

$$T_s = \frac{4}{\varepsilon\omega_n} \tag{23}$$

From the response of the closed-loop induction motor drive with ST-FLC as in Table 4, the value of percent overshoot and settling time are:

$$T_s = 0.293s$$
$$OS\% = 0.0714\%$$

From the value of $OS\%$ we can get the value of damping ratio ζ using equation (23).

$$\zeta = \frac{-\ln(OS\%/100)}{\sqrt{\pi^2 + In^2(OS\%/100)}}$$
$$\varepsilon = \frac{-\ln(0.0714\%/100)}{\sqrt{\pi^2 + In^2(0.0714\%/100)}} = 0.917$$

With the value of ζ and T_s we can get the value of ω_n using equation (24).

$$T_s = \frac{4}{\varepsilon\omega_n} = 0.293 = \frac{4}{0.917\omega_n}$$
$$0.917 \times 0.293\omega_n = 4$$
$$\omega_n = 14.887$$

Now we can substitute the values of ω_n and ε in the general equation of the second order system (equation 21).

$$G(s) = \frac{\omega_n^2}{s^2 + 2\varepsilon\omega_n s + \omega_n^2} = \frac{221.64}{s^2 + 27.3s + 221.64.}$$

This the second order equation representing the closed loop IM drive with ST-FLC speed controller. Now, this transfer function can be analyzed to determine the system stability.

Solving the poles of this transfer function we obtain:

$$-13.6500 + 5.9429i - 13.6500 - 5.9429i$$

It has two poles with negative real parts and no positive poles which means the system is stable. In addition, the root locus of the system has been plotted as shown in Fig. 11 which shows two real poles in the left-half of the S-plane and no matter how the poles increased the poles will remains in the negative left half which means the system stable even if

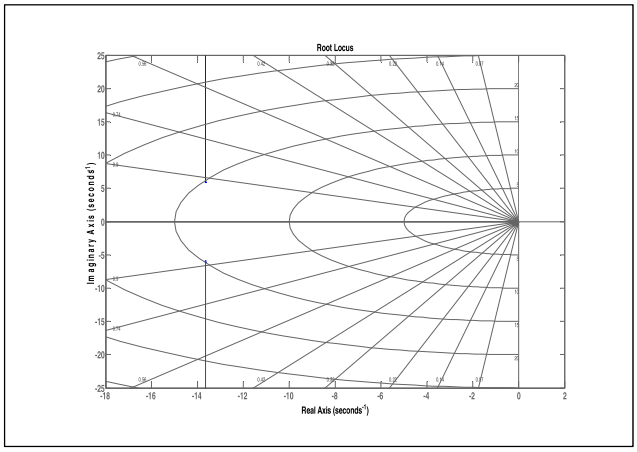

FIGURE 11. Root locus plot of the closed loop transfer function.

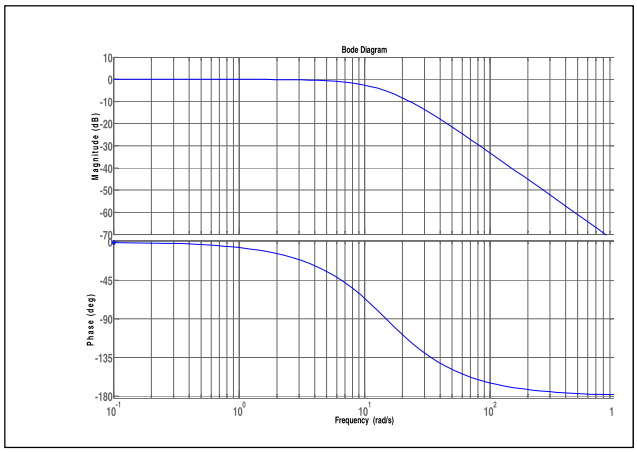

FIGURE 12. Bode plot of the closed loop transfer function of the system (phase and magnitude).

the poles values increased. Moreover, the bode plot response of the transfer function is shown in Fig. 12. From the bode, the phase plot never cross the 180° which means the gain margin is infinity, hence the system will be always stable.

VI. PEXPERIMENTAL SETUP AND RESULT

The experimental setup was done in the Electrical Vehicles Drives Laboratory. The hardware structure of the control system consisted of two interconnected modules: dSPACE DS 1104 and an interface drive board. The dSPACE DS 1104 reads the feedback currents, the speed encoder and finally generates the required switching signals to drive the IM. Overall, the drive system consisted of a workstation, dSPACE DS 1104, FPGA module, gate drives, VSI, current sensor, encoder, IM and DC machine as shown in Fig. 13.

The performance comparison of ST-FLC and FLC were done experimentally in order to validate the robustness and superiority of the proposed ST-FLC controller. The success of the hardware implementation confirmed the workability of the proposed algorithm in real time. Similar fuzzy parameters such as scaling factors, membership function and fuzzy rules were employed with both controllers in order to investigate performance improvement. Similar testing procedures were carried out in the simulation and hardware implementation.

A. NO LOAD OPERATION

The speed performance of both FLC and ST-FLC at rated forward and reverse speed operations are presented in Fig. 14 (a) and (b). Both controllers showed consistent performance in forward and reverse speed operations. The obtained results confirmed the workability of the ST-FLC and validated the simulations results. The speed characteristics comparison of ST-FLC and FLC at rated forward speed operations is summarized in Table 4. Similar to the simulation results, ST-FLC produced superior performance compared to FLC in terms of settling time, rise time and percent overshoot. ST-FLC recorded faster rise time and settling time, and lower overshoot response compared to FLC.

The rated speed response and currents response for ST-FLC and FLC are presented in Fig. 15. ST-FLC recorded better response for both speed and currents which confirmed the influence of output scaling factors on speed and torque performance. According to the obtained results, ST-FLC produced faster current response in comparison to FLC. Similar behavior was observed for the phase A motor stator current with ST-FLC. The current remained constant until the speed reached a steady state condition.

In addition, torque and current performance were analyzed and compared for ST-FLC and FLC. ST-FLC recorded

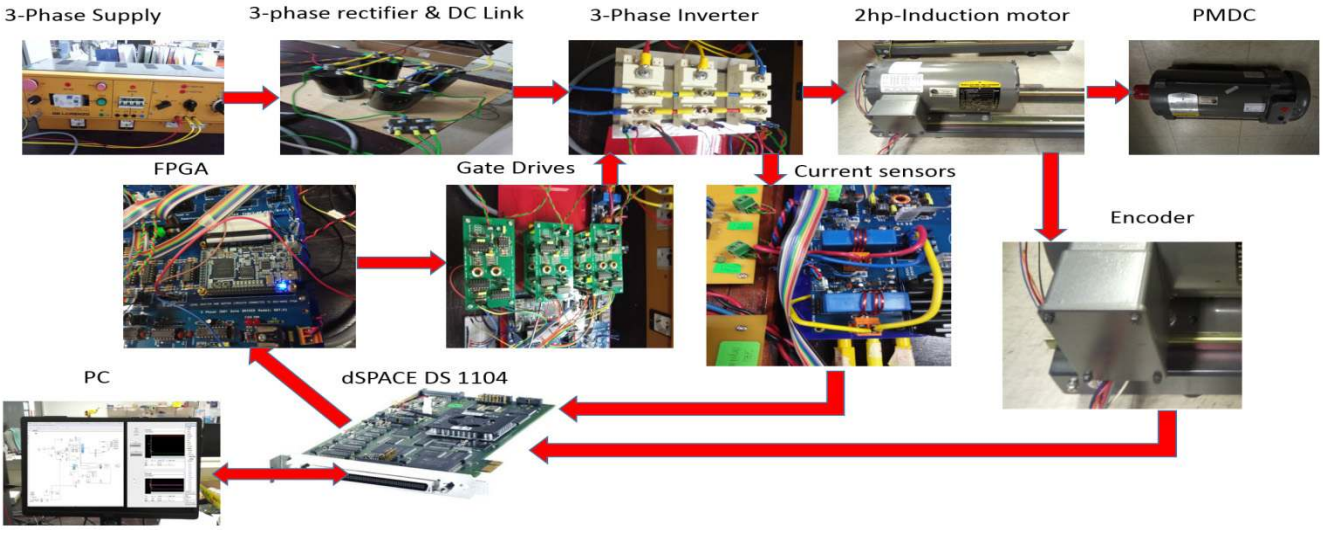

FIGURE 13. Overall experimental setup of vector control of induction motor drives with fuzzy logic speed controller.

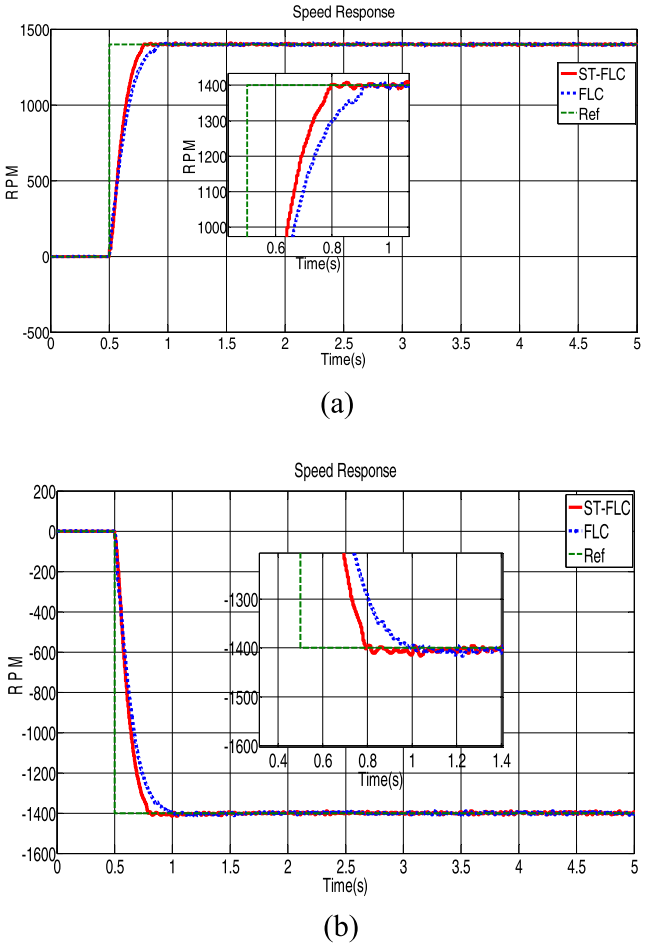

FIGURE 14. Speed performance comparison of FLC and ST-FLC at rated speed.

TABLE 4. Speed performance comparison of FLC and ST-FLC at rated speed.

state	Measures	FLC		ST-FLC	
		Sim	Exp	Sim	Exp
Forward	Settling time (s)	0.3238	0.42	0.293	0.31
	Rise time (s)	0.2412	0.268	0.17082	0.1898
	Overshoot (%)	0.2857	0.443	0.0714	0.137
Reverse	Settling time (s)	0.432	0.48	0.3352	0.35
	Rise time (s)	0.2457	0.273	0.177268	0.1948
	Overshoot (%)	0.2643	0.4371	0.0714	0.1543

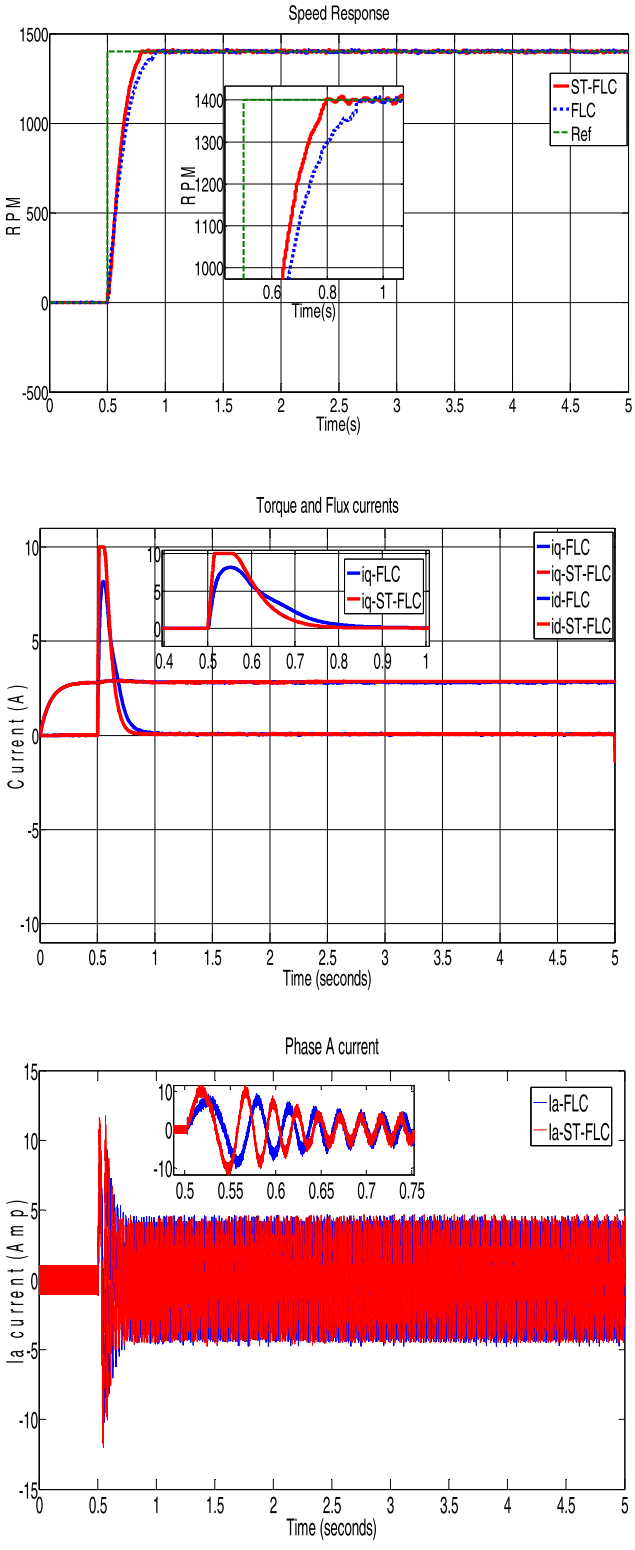

FIGURE 15. Performance comparison of speed, torque and currents at 1400rpm.

smaller ripples for torque and phase current in comparison to FLC. In order to compare the performance of the real stator current characteristic for both controllers, Total Harmonics Distortion (THD) measurement was performed for the phase A stator current. Based on the results, the harmonics generated by the FLC was 0.97% higher than the THD produced by ST-FLC.The experimental results recorded higher THD for both ST-FLC and FLC compared to the simulation results. The THD for the experimental results are 2.19% and 2.97%

TABLE 5. THD comparison of phase a current for FLC and ST-FLC.

Controller	THD%	Fundamental value
FLC	6.50%	2.83
ST-FLC	5.53%	2.864

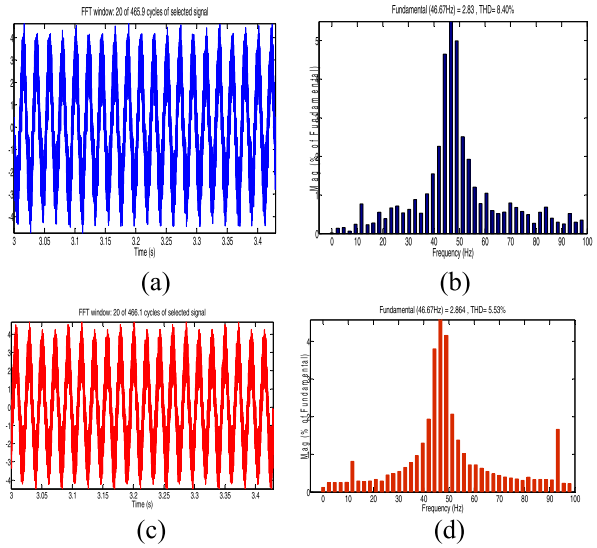

FIGURE 16. IA current THD analysis. (a) FTT window FLC. (b) THD FLC. (c) FTT window ST-FLC. (d) THD ST-FLC.

higher compared to the corresponding simulation results for ST-FLC and FLC. This can be attributed to the high current ripples due to the accuracy of the real current signals sensed by the current transducers, the accuracy of the speed encoder and noise from the hardware. This situation was not encountered during simulation testing due to the ideal model of the speed feedback sensor and current transducer.

B. LOAD OPERATIONS

In order to empirically verify the effectiveness of the controllers towards load rejection capabilities, they were tested under loaded conditions. The IM was coupled to the DC generator and connected to a resistive load bank. The load disturbance was applied at 2.5s. Fig. 17 shows the speed performance of ST-FLC and FLC at full load with rpm. ST-FLC had better load disturbance rejection capabilities. ST-FLC recorded smaller speed drops and faster recovery times in comparison to FLC. At rated speed (1400 rpm) and full load, the ST-FLC recorded a 130 rpm speed drop compared to 155 rpm for FLC. ST-FLC showed a faster recovery time of 0.205s, while FLC recovered in 0.356s at the same speed operation. ST-FLC improved the performance of the drive by a 25 rpm reduction in speed drop and had a 0.151s faster recovery time over the standard FLC.

VII. EXECUTION TIME

The significance of the proposed ST-FLC is shown by its simplicity where less computational burden is produced. This

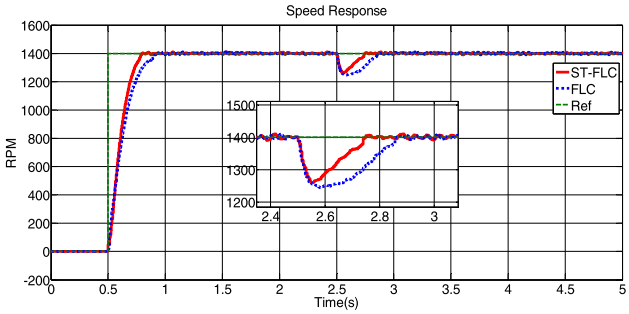

FIGURE 17. Speed performance comparison of FLC-FLC and ST-FLC at rated speed (1400rpm).

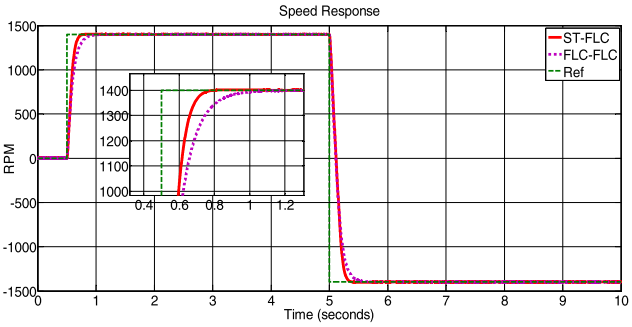

FIGURE 18. Load disturbance comparison of FLC and ST-FLC at full load and rated speed.

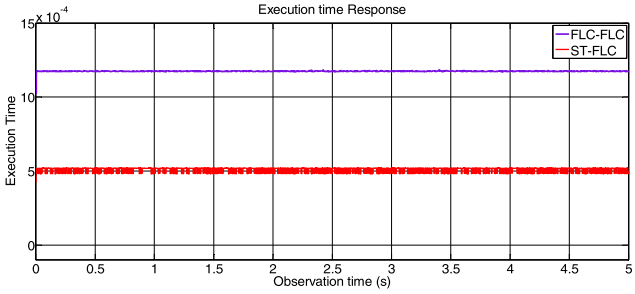

FIGURE 19. Computational time comparison of FLC-FLC and ST-FLC.

is proved by implementing a self-tuning method proposed in [19] which utilized simplified fuzzy rules to tune the output scaling factor of the main FLC, we referred it as (FLC-FLC) to differentiate between it and our proposed ST-FLC. In this FLC-FLC method, the output scaling factor of the main speed FLC is tuned with the help of designed simplified fuzzy rules based on input speed error and input change of speed error.

Further analysis is done based on the execution time of the system. The performance comparison of speed response at 1400 rpm for FLC-FLC and our method ST-FLC is presented in Fig. 16. As can be seen from the results, the ST-FLC has better performance compared to the FLC-FLC in both transient and steady state operations.

In addition, with the help of dSPACE control desk the execution times (computational burden) of both ST-FLC and FLC-FLC were measured as shown in Fig. 18. FLC-FLC produced higher execution time compared to the ST-FLC where 0.5 millisecond and 1.2 millisecond were recorded for ST-FLC and FLC-FLC. The higher execution time of the

TABLE 6. Induction motor specifications.

Parameter	Value
Rated Voltage	380 Vac
Poles	4
Frequency	50Hz
Rated Speed	1430 rpm
Stator Resistance	3.45 Ω
Rotor Resistance	3.6141 Ω
Stator Inductance	0.3246 H
Rotor Inductance	0.3252 H
Magnetizing Inductance	0.3117 H
Inertia	0.02 kgm^2
Viscous Friction	0.001 Nm/(rad/s)

system increase the computational burden for experimental testing where it requires bigger sampling time which will result in degraded performance. The high computational burden produced by FLC-FLC is due to the additional rules used to tune output SF of main FLC, because the fuzzy system has high computational burden to the system. Therefore, unlike other self-tuning method, this proposed method introduced simple but effective ST-FLC which can improve the system performance and reduce the system computational burden.

VIII. CONCLUSION

In this paper, a standard 9 rule FLC was utilized to control the speed of an induction motor drive. In order to enhance performance, a simple ST-FLC consisting of a self-tuning mechanism to tune the output scaling factor was proposed. The simple self-tuning mechanism utilized a mathematical algorithm to adjust the output scaling factor online accordingly based on the input change of error. The effectiveness and workability of the proposed ST- FLC was then evaluated based on simulation and hardware results. Various performance measures such as settling time, overshoot and rise time were used to compare the performance of both controllers under no load and load conditions. Based on the obtained performance comparison, the proposed ST-FLC was found to be superior over the standard FLC. During load analysis, ST-FLC experienced better load disturbance rejection capability with faster recovery times and a smaller drop in speed. Less harmonics content was generated with ST-FLC for stator currents response analysis. In addition, the proposed method is stable for all operating condition and produces less computational burden compared to FLC-FLC tuning method.

APPENDIX A

See Table VI.

REFERENCES

[1] S. A. Odhano, R. Bojoi, A. Boglietti, . G. Ro u, and G. Griva, "Maximum efficiency per torque direct flux vector control of induction motor drives," *IEEE Trans. Ind. Appl.*, vol. 51, no. 6, pp. 4415–4424, Nov./Dec. 2015.

[2] B. Chen, W. Yao, F. Chen, and Z. Lu, "Parameter sensitivity in sensorless induction motor drives with the adaptive full-order observer," *IEEE Trans. Ind. Electron.*, vol. 62, no. 7, pp. 4307–4318, Jul. 2015.

[3] R. Krishnan and F. C. Doran, "Study of parameter sensitivity in high-performance inverter-fed induction motor drive systems," *IEEE Trans. Ind. Appl.*, vol. IA-23, no. 4, pp. 623–635, Jul. 1987.

[4] R. Krishnan and A. S. Bharadwaj, "A review of parameter sensitivity and adaptation in indirect vector controlled induction motor drive systems," *IEEE Trans. Power Electron.*, vol. 6, no. 4, pp. 695–703, Oct. 1991.

[5] L. Zarri, M. Mengoni, Y. Gritli, A. Tani, F. Filippetti, G. Serra, and D. Casadei, "Detection and localization of stator resistance dissymmetry based on multiple reference frame controllers in multiphase induction motor drives," *IEEE Trans. Ind. Electron.*, vol. 60, no. 8, pp. 3506–3518, Aug. 2013.

[6] Y. A. Al-Turki and H. Al-Umari, "Application of the reference frame theory to the dynamic analysis of a three-phase induction motor fed from a single-phase supply," *Electr. Power Syst. Res.*, vol. 53, no. 3, pp. 149–156, Mar. 2000.

[7] R.-J. Wai, C.-M. Lin, and C.-F. Hsu, "Adaptive fuzzy sliding-mode control for electrical servo drive," *Fuzzy Sets Syst.*, vol. 143, no. 2, pp. 295–310, Apr. 2005.

[8] F. F. M. El-Sousy, "Adaptive dynamic sliding-mode control system using recurrent RBFN for high-performance induction motor servo drive," *IEEE Trans Ind. Informat.*, vol. 9, no. 4, pp. 1922–1936, Nov. 2013.

[9] A. V. R. Teja, C. Chakraborty, S. Maiti, and Y. Hori, "A new model reference adaptive controller for four quadrant vector controlled induction motor drives," *IEEE Trans. Ind. Electron.*, vol. 59, no. 10, pp. 3757–3767, Oct. 2012.

[10] M. N. Uddin, Z. R. Huang, and A. B. M. S. Hossain, "Development and implementation of a simplified self-tuned neuro–fuzzy-based IM drive," *IEEE Trans. Ind. Appl.*, vol. 50, no. 1, pp. 51–59, Jan./Feb. 2014.

[11] N. Bounar, A. Boulkroune, F. Boudjema, M. M'Saad, and M. Farza, "Adaptive fuzzy vector control for a doubly-fed induction motor," *Neurocomputing*, vol. 151, no. 2, pp. 756–769, Mar. 2015.

[12] M. A. Hannan, J. A. Ali, A. Hussain, F. H. Hasim, U. A. U. Amirulddin, M. N. Uddin, and F. Blaabjerg, "A quantum lightning search algorithm-based fuzzy speed controller for induction motor drive," *IEEE Access*, vol. 6, pp. 1214–1223, 2017.

[13] Z. Tir, O. P. Malik, and A. M. Eltamaly, "Fuzzy logic based speed control of indirect field oriented controlled double star induction motors connected in parallel to a single six-phase inverter supply," *Electr. Power Syst. Res.*, vol. 134, pp. 126–133, May 2016.

[14] J. A. Ali, M. A. Hannan, A. Mohamed, and M. G. M. Abdolrasol, "Fuzzy logic speed controller optimization approach for induction motor drive using backtracking search algorithm," *Measurement*, vol. 78, pp. 49–62, Jan. 2016.

[15] M. Uddin and M. Hafeez, "FLC-based DTC scheme to improve the dynamic performance of an IM drive," *IEEE Trans. Ind. Appl.*, vol. 48, no. 2, pp. 823–831, Mar./Apr. 2012.

[16] S. M. Gadoue, D. Giaouris, and J. W. Finch, "MRAS sensorless vector control of an induction motor using new sliding-mode and fuzzy-logic adaptation mechanisms," *IEEE Trans. Energy Convers.*, vol. 25, no. 2, pp. 394–402, Jun. 2010.

[17] M. H. N. Talib, Z. Ibrahim, N. A. Rahim, A. S. A. Hasim, and H. Zainuddin, "Performance improvement of induction motor drive using simplified FLC method," in *Proc. 16th Int. Power Electron. Motion Control Conf. Expo.*, Sep. 2014, pp. 707–712.

[18] F. Betin, A. Sivert, A. Yazidi, and G. A. Capolino, "Determination of scaling factors for fuzzy logic control using the sliding-mode approach: Application to control of a DC machine drive," *IEEE Trans. Ind. Electron.*, vol. 54, no. 1, pp. 296–309, Feb. 2007.

[19] M. H. N. Talib, Z. Ibrahim, Z. Rasin, J. M. Lazi, and S. N. M. Isa, "Simplified self-tuning fuzzy logic speed controller for induction motor drive," in *Proc. IEEE Int. Conf. Power Energy (PECon)*, Nov. 2016, pp. 188–193.

[20] M. Masiala, B. Vafakhah, J. Salmon, and A. M. Knight, "Fuzzy self-tuning speed control of an indirect field-oriented control induction motor drive," *IEEE Trans. Ind. Appl.*, vol. 44, no. 6, pp. 1732–1740, Nov. 2008.

[21] N. S. Y. Farah, M. H. N. Talib, Z. Ibrahim, Z. Rasin, and Z. I. Rizman, "Experimental investigation of different rules size of fuzzy logic controller for vector control of induction motor drives," *J. Fundam. Appl. Sci.*, vol. 10, no. 6, pp. 1696–1717, 2018.

[22] R. K. Mudi and N. R. Pal, "A robust self-tuning scheme for PI- and PD-type fuzzy controllers," *IEEE Trans. Fuzzy Syst.*, vol. 7, no. 1, pp. 2–16, Feb. 1999.

[23] Z. Mekrini and S. Bri, "Performance of an indirect field oriented control for asynchronous machine," *Int. J. Eng. Technol.*, vol. 8, no. 2, pp. 726–733, Apr. 2016.

[24] B. K. Bose, *Modern Power Electronics and AC Drives*, vol. 123. Upper Saddle River, NJ, USA: Prentice-Hall, 2002.
[25] M. Ahmad, *High Performance AC Drives: Modelling Analysis and Control*. Berlin, Germany: Springer-Verlag, 2010.
[26] J.-L. Chameau and J. C. Santamarina, "Membership functions I: Comparing methods of measurement," *Int. J. Approx. Reasoning*, vol. 1, no. 3, pp. 287–301, 1987.
[27] J. Zhao and B. K. Bose, "Evaluation of membership functions for fuzzy logic controlled induction motor drive," in *Proc. IEEE 28th Annu. Conf. Ind. Electron. Soc.*, vol. 1, Nov. 2002, pp. 229–234.
[28] A. Rubaai, D. Ricketts, and M. D. Kankam, "Laboratory implementation of a microprocessor-based fuzzy logic tracking controller for motion controls and drives," *IEEE Trans. Ind. Appl.*, vol. 38, no. 2, pp. 448–456, Mar. 2002.
[29] F. Betin and G.-A. Capolino, "Sliding mode control for an induction machine submitted to large variations of mechanical configuration," *Int. J. Adapt. Control Signal Process.*, vol. 21, nos. 8–9, pp. 745–763, 2007.
[30] S. Y. Lee and H. S. Cho, "A fuzzy controller for an aeroload simulator using phase plane method," *IEEE Trans. Control Syst. Technol.*, vol. 9, no. 6, pp. 791–801, Nov. 2001.
[31] H. Sugimoto and E. Ohno, "A new induction motor drive system with linear transfer function," *Elect. Eng. Jpn.*, vol. 103, no. 1, pp. 47–55, 1983.
[32] N. S. Nise, *Control Systems Engineering*, 6th ed. Pomona, CA, USA: Wiley, 2007.

NABIL FARAH was born in Yemen, in 1988. He received the bachelor's degree in electrical engineering (power electronics and drives) from the Universiti Teknikal Malaysia Melaka, in 2015, and the master's degree in electrical engineering from the Universiti Teknikal Malaysia Melaka, where he is currently pursuing the Ph.D. degree. His current research interests include self-tuning fuzzy logic controller of AC motor drives and predictive control of induction motor drives.

MD. HAIRUL NIZAM TALIB was born in Malaysia, in 1976. He received the B.S. degree in electrical engineering from the Universiti Teknologi Malaysia (UTM), Johor Bahru, Malaysia, in 1999, the M.S. degree in electrical engineering from the University of Nottingham, Nottingham, U.K., in 2005, and the Ph.D. degree from the Universiti Teknikal Malaysia Melaka (UTeM), Malaysia, in 2016, where he is currently a Senior Lecturer. His main research interests include power electronics, fuzzy logic control, and motor drives.

NOR SHAHIDA MOHD SHAH received the B.Eng. degree from the Tokyo Institute of Technology, the master's degree (Hons.) from the University of Malaya, and the Ph.D. degree from Osaka University, in 2000, 2003, and 2012, respectively. Since 2004, she has been with Universiti Tun Hussein Onn Malaysia. Her research interests include optical fiber devices, optical communication, antenna and propagation, and wireless communication.

QAZWAN ABDULLAH was born in Taiz, Yemen. He received the bachelor's and master's degrees in electrical and electronic engineering from Universiti Tun Hussein Onn Malaysia (UTHM), in 2013 and 2015, respectively, where he is currently pursuing the Ph.D. degree. His research interests include control systems, wireless technology, and microwaves.

ZULKIFILIE IBRAHIM was born in Malaysia, in 1966. He received the B.Eng. degree from the University of Technology (UTM), Malaysia, in 1989, and the Ph.D. degree from Liverpool John Moores University, U.K., in 1999. He is currently a Professor with the Universiti Teknikal Malaysia Melaka (UTeM), Malaysia. His main research interests include power electronics, fuzzy logic control, embedded system design, and electric motor drives.

JURIFA BINTI MAT LAZI received the bachelor's and M.Sc. degrees in electrical engineering from Universiti Teknologi Malaysia, in 2001 and 2003, respectively, and the Ph.D. degree from the Universiti Teknikal Malaysia Melaka, in 2016. Since 2001, she has been serving as an Academic Staff of the Universiti Teknikal Malaysia Melaka (UTeM), where she is currently a Senior Lecturer and the Head of Industrial Training Coordinator with the Faculty of Electrical Engineering. Her research interests include machine drives, especially in sensorless, and PMSM drives, power electronics, and power systems.

AUZANI JIDIN (M'09) received the B.Eng., M.Eng., and Ph.D. degrees in power electronics and drives from Universiti Teknologi Malaysia (UTM), Malaysia, in 2002, 2004, and 2011, respectively. He is currently a Lecturer with the Department of Power Electronics and Drives, Faculty of Electrical Engineering, Universiti Teknikal Malaysia Melaka (UTeM), Malaysia. His research interests include the field of power electronics, motor drive systems, FPGA, and DSP applications.